

Somatic alteration and depleted nuclear expression of BAP1 in human esophageal squamous cell carcinoma

Takahiro Mori,¹ Makiko Sumii,¹ Fumiyoshi Fujishima,² Kazuko Ueno,³ Mitsuru Emi,⁴ Masao Nagasaki,³ Chikashi Ishioka⁵ and Natsuko Chiba⁶

¹Tohoku Community Cancer Services Program, Tohoku University Graduate School of Medicine, Sendai; ²Department of Pathology, Tohoku University Hospital, Sendai; ³Department of Integrative Genomics, Tohoku Medical Megabank Organization, Tohoku University, Sendai, Japan; ⁴Thoracic Oncology Program, University of Hawaii Cancer Center, Honolulu, Hawaii, USA; Departments of ⁵Clinical Oncology; ⁶Cancer Biology, Institute of Development, Aging and Cancer, Tohoku University, Sendai, Japan

Key words

BAP1, deubiquitinase, esophageal squamous cell carcinoma, gene expression profiling, somatic mutation

Correspondence

Takahiro Mori, Tohoku Community Cancer Services Program, Tohoku University Graduate School of Medicine, 1-1 Seiryomachi, Aoba-ku, Sendai, Japan 980-8574. Tel: +81-22-717-7087; Fax: +81-22-717-7896; E-mail: tamori@med.tohoku.ac.jp

Funding Information

This work was supported by a grant-in-aid for scientific research C, #25462010, from the Ministry of Education, Culture, Sports, Science and Technology, Japan and Program for interdisciplinary research in Frontier Research Institute for Interdisciplinary Sciences (FRIS), Tohoku University.

Received December 27, 2014; Revised May 27, 2015; Accepted June 11, 2015

Cancer Sci 106 (2015) 1118–1129

doi: 10.1111/cas.12722

BRCAl-associated protein 1 (BAP1) was identified as a protein that binds to the amino-terminal RING domain of BRCA1.⁽¹⁾ It is a nuclear deubiquitinating enzyme with ubiquitin carboxyl hydrolase (UCH) activity that regulates cell growth in a UCH-dependent but BRCA1-independent manner.⁽²⁾ BAP1 contains two nuclear localization signals; nuclear localization is required for its tumor suppressor function.^(3–5) BAP1 is frequently mutated in metastasizing uveal melanomas as well as in malignant pleural mesothelioma, renal cell carcinoma and intrahepatic cholangiocarcinoma.^(6–11) Furthermore, a number of germline BAP1 mutations have been reported to predispose to susceptibility to several tumors: the so-called BAP1 cancer syndrome.^(12–18) This suggests that BAP1 mutation can occur in various types of cancers, including as yet unreported malignant diseases. We previously reported that chromosome 3p21, where BAP1 is located, is frequently deleted in esophageal squamous cell carcinoma (ESCC), although BAP1 mutation had not been reported in this type of cancer.^(19,20) In addition, we applied MLPA analysis to explore copy number alteration at the BAP1 locus.

BRCA1-associated protein 1 (BAP1) is a deubiquitinating enzyme that is involved in the regulation of cell growth. Recently, many somatic and germline mutations of BAP1 have been reported in a broad spectrum of tumors. In this study, we identified a novel somatic non-synonymous BAP1 mutation, a phenylalanine-to-isoleucine substitution at codon 170 (F170I), in 1 of 49 patients with esophageal squamous cell carcinoma (ESCC). Multiplex ligation-dependent probe amplification (MLPA) of BAP1 gene in this ESCC tumor disclosed monoallelic deletion (LOH), suggesting BAP1 alterations on both alleles in this tumor. The deubiquitinase activity and the auto-deubiquitinase activity of F170I-mutant BAP1 were markedly suppressed compared with wild-type BAP1. In addition, wild-type BAP1 mostly localizes to the nucleus, whereas the F170I mutant preferentially localized in the cytoplasm. Microarray analysis revealed that expression of the F170I mutant drastically altered gene expression profiles compared with expressed wild-type BAP1. Gene-ontology analyses indicated that the F170I mutation altered the expression of genes involved in oncogenic pathways. We found that one candidate, TCEAL7, previously reported as a putative tumor suppressor gene, was significantly induced by wild-type BAP1 as compared to F170I mutant BAP1. Furthermore, we found that the level of BAP1 expression in the nucleus was reduced in 44% of ESCC examined by immunohistochemistry (IHC). Because the nuclear localization of BAP1 is important for its tumor suppressor function, BAP1 may be functionally inactivated in a substantial portion of ESCC. Taken together, BAP1 is likely to function as a tumor suppressor in at least a part of ESCC.

Here, we sought to clarify whether genetic alterations in BAP1 are found in ESCC and play an important role in esophageal carcinogenesis.

Materials and Methods

Patients. This study was approved by the Ethics Committee of Tohoku University Graduate School of Medicine (numbers: 2013-1-70, 2013-1-116) and all patients enrolled in this study gave written informed consent for genome analysis, except those who had undergone esophagectomy before 2001, when the Japanese Government officially announced guidelines for human genome analysis. Genomic study was approved for the above cases only under the condition of unlinked anonymity. Forty-nine patients were enrolled in this genome-analysis study. Genomic DNA was extracted from frozen tissues in 48 patients and from formalin-fixed paraffin-embedded (FFPE) normal and cancerous tissues in 1 patient; all of 49 tumors were pathologically diagnosed as ESCC (Table 1). Genomic DNA extracted from frozen normal epithelia and tumor tissues from 27 patients

Table 1. Clinical and pathological data of patients of esophageal squamous cell carcinoma in this study

Case number	Sex	Age at treatment	Material	Stage (TNM)	Prognosis (Ms, months)	CNV at <i>BAP1</i> in tumor	<i>BAP1</i> somatic mutation	Nuclear <i>BAP1</i> (IHC)
TUH-20	M	59	FFPE	T3N1M0	2Ms, died from cancer	NE	NE	Negative*
TUH-22	F	72	FFPE	T2N0M0	71.3Ms, survives	NE	NE	Negative
TUH-25	M	59	FFPE	T3N1M0	8.5Ms, died from cancer	NE	NE	Positive
TUH-30	M	37	FFPE	T3N1M0	21.2Ms, died from cancer	NE	NE	Negative*
TUH-31	M	69	FFPE	T2N1M0	67.3Ms, survives	NE	NE	Negative*
TUH-34	F	61	FFPE	T1N1M0	9.1Ms, died from cancer	NE	NE	Negative
CI-103	M	59	Frozen tissues	NA	NA	NE	No	NE
CI-107	M	33	Frozen tissues	NA	NA	ex11–17 loss	No	NE
CI-108	M	70	Frozen tissues	NA	NA	NE	No	NE
CI-109	F	64	Frozen tissues	NA	NA	NE	No	NE
CI-110	F	61	Frozen tissues	NA	NA	NE	No	NE
CI-111	M	60	Frozen tissues	NA	NA	ex1–6, ex12–17 loss	No	NE
CI-112	M	57	Frozen tissues	NA	NA	ex1, 4, 5, 12, 13, 14, 16, 17 loss	No	NE
CI-113	M	67	Frozen tissues	NA	NA	No CNV	No	NE
CI-114	M	57	Frozen tissues	NA	NA	ex1, 5, 12, 13, 14, 16, 17 loss	No	NE
CI-116	M	55	Frozen tissues	NA	NA	NE	No	NE
CI-117	M	66	Frozen tissues	NA	NA	NE	No	NE
CI-118	M	54	Frozen tissues	NA	NA	NE	No	NE
CI-119	M	55	Frozen tissues	NA	NA	NE	No	NE
CI-120	M	61	Frozen tissues	NA	NA	ex1, 4, 5, 6, 8, 10, 11, 12, 13, 14, 16, 17 loss	No	NE
CI-122	M	45	Frozen tissues	NA	NA	NE	No	NE
CI-123	M	70	Frozen tissues	NA	NA	ex1-17 loss	No	NE
CI-124	M	76	Frozen tissues	NA	NA	No CNV	No	NE
CI-125	M	63	Frozen tissues	NA	NA	ex1–17 loss	F170I	NE
CI-126	NA	NA	Frozen tissues	NA	NA	No CNV	No	NE
CI-128	M	67	Frozen tissues	NA	NA	No CNV	No	NE
TU-204	M	66	Frozen tissues	T4N1M1	16.4Ms, died from cancer	NE	No	NE
TU-205	M	60	Frozen tissues	T3N1M0	16.1Ms, died from cancer	NE	No	NE
TU-206	M	75	Frozen tissues	T4N1M0	18.4Ms, died from cancer	NE	No	Positive
TU-207	M	69	Frozen tissues	T3N1M0	5.3Ms, died from cancer	NE	No	NE
TU-209	M	74	Frozen tissues	T2N1M0	90.7Ms, died from pneumonia	NE	No	NE
TU-210	M	67	Frozen tissues	T1N1M1	8.3Ms, died from cancer	ex1–17 loss	No	Negative
TU-211	M	59	Frozen tissues	T4N0M0	57.7Ms, died from cancer	No CNV	No	Positive
TU-212	M	62	Frozen tissues	T4N1M0	3.2Ms, died from cancer	NE	No	NE
TU-214	M	66	Frozen tissues	T3N1M1	6.6Ms, died from cancer	ex1 loss	No	Positive
TU-215	M	75	Frozen tissues	T3N0M0	8.8Ms, died from cancer	NE	No	Negative*
TU-217	M	65	Frozen tissues	T3N1M0	144.7Ms, survives	NE	No	Negative
TU-218	M	58	Frozen tissues	T4N1M0	9.5Ms, died from cancer	No CNV	No	Positive
TU-219	M	54	Frozen tissues	NA	NA	NE	No	NE
TU-220	M	64	Frozen tissues	T3N1M0	108.6Ms, died from other cancer	ex1–17 loss	No	Positive
TU-221	F	56	Frozen tissues	T3N1M0	15.9Ms, died from AMI	No CNV	No	Positive
TU-222	M	67	Frozen tissues	T4N1M0	153.2Ms, survives	No CNV	No	Positive
TU-223	M	89	Frozen tissues	T3N1M0	21.2Ms, died from pneumonia	NE	No	Negative
TU-224	M	66	Frozen tissues	T2N0M0	139.4Ms, survives	ex1 loss	No	Negative
TU-225	M	77	Frozen tissues	T2N1M0	3.4Ms, died from MOF	NE	No	Negative
TU-227	M	74	Frozen tissues	T2N1M0	37.1Ms, died from cancer	No CNV	No	Negative
TU-228	M	75	Frozen tissues	T3N1M1	16.0Ms, died from cancer	No CNV	No	Negative
TU-229	M	46	Frozen tissues	T4N1M0	11.1Ms, died from cancer	No CNV	No	Positive
TU-230	M	76	Frozen tissues	T1N0M0	138.7Ms, survives	ex1–17 loss	No	Negative
TU-231	M	67	Frozen tissues	T2N1M1	5.4Ms, died from cancer	ex4–17 loss	No	Negative
TU-232	F	74	Frozen tissues	T3N0M0	7.5Ms, died from cancer	No CNV	No	Positive

Table 1 (continued)

Case number	Sex	Age at treatment	Material	Stage (TNM)	Prognosis (Ms, months)	CNV at BAP1 in tumor	BAP1 somatic mutation	Nuclear BAP1 (IHC)
TU-233	NA	NA	Frozen tissues	NA	NA	ex1–16 loss	No	NE
TU-234	M	76	Frozen tissues	T4N1M0	127.2Ms, died from other cancer	No CNV	No	Positive
TU-235	M	71	Frozen tissues	T1N0M0	62.8Ms, died from pneumonia	NE	No	NE
ST-010	M	77	WhiteBlood cells and FFPE	T1N0M0	127.5Ms, survives	NE	NE	Positive
ST-033	M	53	White Blood cells and FFPE	T3N1M0	82.8Ms, died from ML	NE	NE	Positive
ST-041	M	67	WhiteBlood cells and FFPE	T2N1M0	98.4Ms, survives	NE	NE	Negative
ST-049	M	74	White Blood cells and FFPE	T1N0M0	75.2Ms, died from cancer	NE	NE	Positive
ST-050	M	54	WhiteBlood cells and FFPE	T2N0M0	58.7Ms, survives	NE	NE	Positive
ST-051	M	63	White Blood cells and FFPE	T1N0M0	107.2Ms, survives	NE	No	Negative*
ST-075	M	59	White blood cells and FFPE	T3N1M0	10.5Ms, died from cancer	NE	NE	Negative
ST-094	M	67	White blood cells and FFPE	T3N1M1b	8.1Ms, died from cancer	NE	NE	Positive
ST-116	M	69	White blood cells and FFPE	T3N1M0	34.3Ms, died from cancer	NE	NE	Negative*
ST-123	M	71	White blood cells and FFPE	T3N1M0	34.8Ms, survives	NE	NE	Positive
ST-145	M	65	White blood cells and FFPE	T1N1M0	102.3Ms, survives	NE	NE	Positive
ST-156	M	65	White blood cells and FFPE	T3N1M0	35.3Ms, survives	NE	NE	Positive
ST-163	M	56	White blood cells and FFPE	T3N1M0	21.3Ms, died from cancer	NE	NE	Negative
ST-166	M	59	White blood cells and FFPE	T3N0M0	14Ms, survives	NE	NE	Positive
ST-169	M	62	White blood cells and FFPE	T2N1M0	1.6Ms, died from AMI	NE	NE	Positive
ST-176	M	58	White blood cells and FFPE	T3N1M0	103.8Ms, survives	NE	NE	Negative*
ST-180	M	67	White blood cells and FFPE	T3N1M0	41.7Ms, survives	NE	NE	Positive
ST-196	F	63	White blood cells and FFPE	T3N0M0	59.0Ms, survives	NE	NE	Positive
ST-213	M	65	White blood cells and FFPE	T3N1M0	96.0Ms, survives	NE	NE	Negative
ST-219	M	60	White blood cells and FFPE	T3N0M0	49.1Ms, died from cancer	NE	NE	Positive
TM109	M	60	FFPE	T3N1M0	8.8Ms, died from cancer	NE	NE	Positive
TM113	M	55	FFPE	T3N1M0	Survives with recurrence	NE	NE	Positive
TM115	F	48	FFPE	T2N1M0	4.9Ms, died from cancer	NE	NE	Positive
TM130	F	44	FFPE	T4N1M0	13.0Ms, died from cancer	NE	NE	Positive
TM131	M	59	FFPE	T4N1M0	Survives	NE	NE	Negative*
TM133	M	68	FFPE	T3N1M0	6.2Ms, died from cancer	NE	NE	Positive

CNV, copy number variation; NA, not available; NE, not examined. The asterisks after IHC-negative indicate cases with cytosolic strong positive-ness.

and formalin-fixed paraffin-embedded tissues from 52 patients were used for copy number variation (CNV) analysis and IHC analysis, respectively.

DNA sequencing. We sequenced all exons as well as flanking 5'- and 3'-untranslated regions of *BAP1* in genomic DNA from

48 surgically resected ESCC and corresponding normal tissues, which were extracted from frozen tissues, by Sanger sequencing. Later, an additional case, diagnosed as BAP1 negative by IHC, was sequenced using DNA extracted from FFPE tissues as described above. Clinical and pathological data of all sam-

ples used in this study are summarized in Table 1. PCR primers are listed in Supplementary Table S1.

Cell line and transfection. HEK-293T cells and U2OS cells were grown in DMEM supplemented with 10% FBS. Cells were transfected with plasmids using Lipofectamine LTX (Invitrogen, Carlsbad, CA, USA).

MLPA analysis. MLPA analysis of genomic DNA for each exon of *BAP1* gene was carried out using SALSA MLPA BAP1 kit P417-B1-1011 BAP1-v03; probe data are described in SALSA MLPA probemix P417-B1 BAP1 (MRC Holland, Amsterdam, the Netherlands). Data analysis was performed following the manufacturer's instruction. The peak areas achieved using *BAP1* specific probes in each sample were first normalized by the average of peak areas achieved by control probes specific for locations from other chromosomes. A corresponding calculation was performed for genomic DNA isolated from peripheral blood of normal individuals. We regarded the average value from the normal control DNA as diploid. A final ratio was then calculated by dividing the value from the patient samples by the average value from the control DNA. If this ratio was below 0.7 (\log_2 ratio below -0.52), the sample was scored to have loss of one copy number (monoallelic loss); if this ratio was below 0.25 (\log_2 ratio below -2), the sample was scored to have loss of two-copy numbers (biallelic loss). In addition, a negative sample (water) was included in each run.

Plasmid construction. For pCY4B-FLAG-BAP1, the *BAP1* sequence was amplified from the cDNA of HEK-293T cells generated using a Transcriptor High-Fidelity cDNA Synthesis kit (Roche Applied Science, Penzberg, Germany). The amplified PCR products were subcloned into pCY4B-FLAG.⁽²¹⁾ pCY4B-FLAG-BAP1-F170I was generated by site-directed mutagenesis to create the amino acid substitution phenylalanine to isoleucine at codon 170. For pCY4B-HA-HCF1-1-380, the *HCF1* sequence was amplified from the cDNA of HEK-293T cells as described above, and was subcloned into pCY4B-HA. pCMV-Myc-ubiquitin has been described previously.⁽²²⁾ All constructs were verified by Sanger sequencing. PCR primers as listed below were used for plasmid constructions:

BAP1-Xho-F; 5'- GACTCGAGATGAATAAGGGCTGGC
TGGAGCTGGAG-3'
BAP1-Not-R; 5'- TCATGCGGCCGCACTGGCGCTTGGC
CTTGTAGGGGCGA-3'
HCF1-Xho-F; 5'- TACTCGAGATGGCTTCGGCCGTGTC
GCCCGCAACTT-3'
HCF1-Not-R; 5'- TCATGCGGCCGCACAGGGAGTTGGT
GTTGGCGGTACCAG-3'.

In vivo ubiquitination assays. An *in vivo* ubiquitination assay was performed as described previously.⁽²³⁾ HEK-293T cells were transfected with the vectors described above, and 2 days after transfection, cells were lysed in boiling buffer (1% SDS in PBS). After heating the lysate for 5 min at 100°C and sonicating to shear the DNA, immunoprecipitations (IP) were performed in 1% Triton X-100, 0.5% SDS, 0.25% sodium deoxycholate, 0.5% BSA, 1 mM EDTA in PBS containing a protease inhibitor cocktail (Sigma, St. Louis, MO, USA) using anti-HA (HA.11 Monoclonal Antibody #MMS-101R; Covance, Princeton, NJ, USA) or anti-BAP1 antibody (sc-28383, Santa Cruz, Dallas, TX, USA) and Protein G Sepharose beads (GE Healthcare, Little Chalfont, UK). Reaction mixtures were incubated at 4°C for 16 h and protein beads were washed twice with the same buffer and twice with 10-fold diluted PBS. Samples were subjected to SDS-PAGE and immunoblotted using

anti-Myc (9E10 sc-40, Santa Cruz), anti-FLAG (monoclonal anti-FLAG M2 antibody, Sigma), anti-HA (anti-HA high affinity #1867423, Roche Applied Science) and anti-BAP1 antibodies. Experiments were independently repeated in triplicate and ubiquitination level was quantified by Image Quant TL (GE Healthcare).

Immunocytochemistry. U2OS cells were transfected with pCY4B-FLAG-BAP1-Wt or -F170I, and fixed for 10 min in PBS-buffered 3% paraformaldehyde and 2% sucrose solution, followed by a 5-min permeabilization on ice in Triton buffer (0.5% Triton X-100 in 20 mM HEPES (pH 7.4), 50 mM NaCl, 3 mM MgCl and 300 mM sucrose). After blocking by PBS containing 3% skimmed milk, cells were incubated with anti-FLAG antibody in PBS 1% BSA for 4 h. After washing with PBS containing 0.05% Tween 20 (PBS-T), cells were incubated with Alexa Fluor 488-conjugated antibody (Molecular Probes, Eugene, OR, USA) in PBS 1% BSA for 30 min. Cells were washed with PBS-T and mounted in mounting medium with DAPI (Vector Laboratories, Burlingame, CA, USA).

Microarray analysis and gene ontology analysis. HEK-293T cells were transiently transfected either with pCY4B-FLAG-BAP1-Wt or -F170I. Forty-eight hours after transfection, cells were collected and total RNA were extracted using ISOGEN (Nippon Gene, Tokyo, Japan). A Whole Human Genome Microarray Kit, 4 × 44K (#G4112F, Agilent, Santa Clara, CA, USA) was hybridized with total cDNA generated from total RNA using a Low Input Quick-Amp Labeling Kit (Agilent) and the signals were analyzed. Each experiment with wild-type BAP1 or F170I mutant was conducted twice. The microarray data were extracted using the GeneSpring version 12.5 (Agilent). The raw data were normalized using quantile normalization and used for heat-map analysis and principal component analysis. Genes were selected by the values of the first component of the vector in principal component analysis, more than 1.428 or less than -1.907 , because *APOL6* (1.428) and *HSPA6* (-1.907) were 1.5-fold differentially expressed between wild-type *BAP1* and the F170I mutant, according to the ratio of averaged expression values in heat-map analysis of two independent F170I mutant and wild-type BAP1 transfections. Then, genes without genome annotation were excluded from the study. The 5840 genes ultimately selected were used for gene ontology analyses by Ingenuity Pathways Analysis (IPA) (<http://www.ingenuity.com>); Tomy Digital Biology, Tokyo, Japan), DAVID KEGG, DAVID BioCartas and DAVID Reactome (DAVID Bioinformatics Resources 6.7; <http://david.abcc.ncifcrf.gov>).

Immunohistochemical staining and pathological evaluation. Surgical specimens were fixed in 10% formalin and representative sections were embedded in paraffin wax. Serial 4- μ m-thick sections from the most representative area of each specimen were deparaffinized in xylene, rehydrated in a graded ethanol series, and then immersed in 3.0% hydrogen peroxide in methanol for 10 min at room temperature (RT) to block endogenous peroxidase activity. For antigen retrieval, the slides were heated for 5 min in 0.01 M citrate buffer (pH 6.0) using an autoclave at 121°C. The slides were incubated in 1% normal rabbit serum for 30 min at RT to reduce non-specific antibody binding. Subsequently, the slides were incubated at 41°C overnight with anti-BAP1 antibody (sc-28383, Santa Cruz, diluted 1/100). The next day, the sections were incubated with biotinylated anti-mouse secondary antibody (Nichirei Biosciences, Tokyo, Japan), then incubated with peroxidase-labeled streptavidin (Nichirei Biosciences) for 30 min at RT. The antigen-antibody complexes were visualized with 3,3'-diaminobenzidine, and the slides were counterstained with

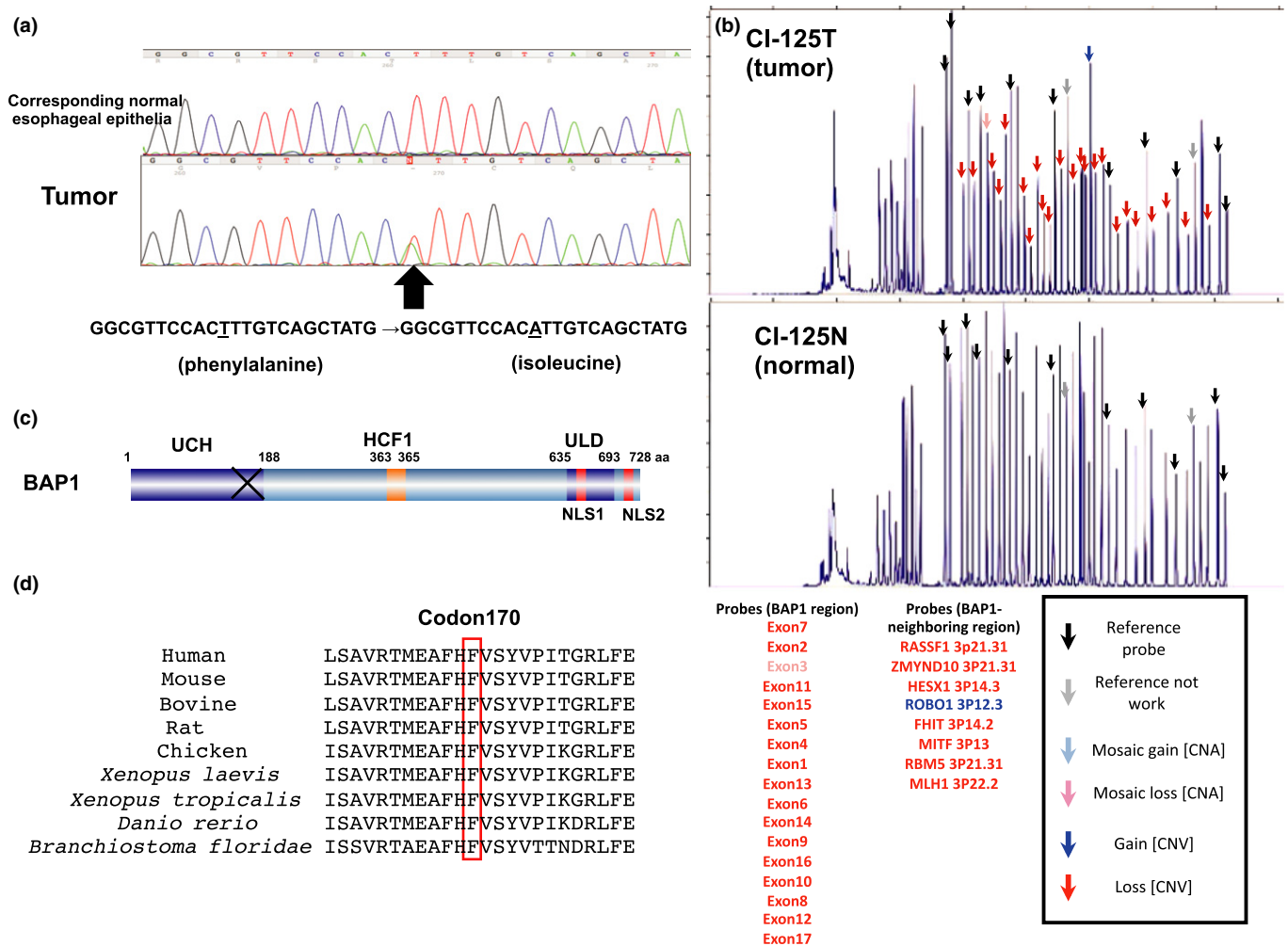


Fig. 1. (a) BAP1 mutation in a patient with esophageal squamous cell carcinoma. In tumor tissue, TTT, encoding phenylalanine, is altered to ATT, encoding isoleucine (arrowhead). A faint peak observed in sequence data of this tumor likely represents contaminated residual non-carcinoma DNA, as indicated by MLPA analysis (b). (b) MLPA data for all 17 exons of BAP1 gene on 3p21.1 are displayed on the x-axis. The table in the (b) also displays peaks of eight control probes, and *RASSF1*, *MYND10*, *HEX1*, *ROBO1*, *FHIT*, *MITF*, *RBMS* and *MLH1* in the BAP1-neighboring region on chromosome 3p. Probe position and peak height in the (b) are described in SALSA MLPA probemix P417-B1 BAP1 (MRC Holland, Amsterdam, the Netherlands). Log₂ ratio of MLPA data for each probe is indicated on the y-axis. (c) Schematic of BAP1 with the F170I mutation. UCH, HCF1, ULD and NLS stand for ubiquitin C-terminal hydrolase domain, HCF1-binding domain, UCH37-like domain and nuclear localization signal, respectively. The F170I substitution is indicated by X. (d) Conservation of BAP1 in the region containing the F170I mutation. Alignment of amino acid sequences from codons 159–182 in human BAP1 and its counterparts in other species as identified by BLAST (<http://www.genome.jp/tools/blast/>). Codon 170 is boxed.

Mayer's hematoxylin, dehydrated in a graded ethanol series, and cleared in xylene.

The staining and pathological findings were evaluated independently by two of the authors (T.M. and F.F.) who were blinded to the patients' clinical data. Tumors were scored as positive or negative depending on whether or not their nuclei stained with BAP1.^(14,24)

Real-time reverse transcription PCR of TCEAL7. To determine the RNA expression level of *TCEAL7* gene, we performed a real time RT-PCR assay; in brief, cDNA created with an iScript Advanced cDNA Synthesis Kit for RT-qPCR (BioRad, Hercules, CA, USA) using total RNA extracted from HEK-293T cells transfected with wild-type BAP1 or F170I-mutant were used as a template, then mixed with Supermixes for PCR and Real-Time PCR (BioRad) and *TCEAL7*-specific primers as well as *GAPDH* primers, and analyzed using the CFX96 Touch Real-Time PCR Detection System (Bio-Rad). Real-time

PCR was performed in triplicate for independent duplicated transfections with either wild-type (Wt) or F170I-mutant BAP1 and the results were analyzed using statistical procedures (SPSS ver.22.0; IBM, Armonk, NY, USA). Primers were used as previously reported.⁽²⁵⁾

Results

Somatic point mutation coupled with monoallelic deletion of BAP1 gene in an esophageal squamous cell carcinoma among those that display frequent LOH at BAP1 locus. Among 49 patients with ESCC examined by direct sequencing, we identified a somatic non-synonymous mutation of BAP1 in an ESCC tumor. This mutation caused an amino acid substitution from phenylalanine to isoleucine at codon 170 (Fig. 1a). MLPA analysis shows that this tumor lost the remaining allele of BAP1 as displayed in Figure 1(b). These results revealed

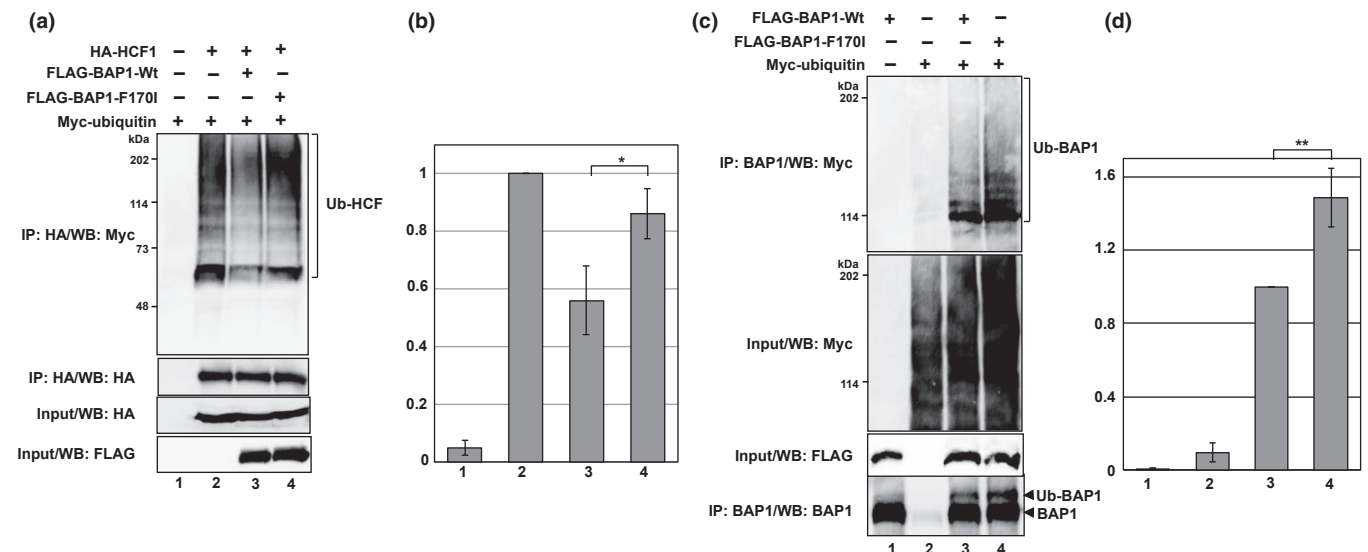


Fig. 2. (a) Deubiquitination of HCF1 by BAP1. Plasmids as described were transfected into HEK-293T cells. Cell extracts were immunoprecipitated with anti-HA antibody, followed by western blot analysis with either anti-Myc or with anti-HA antibody. The expression level of HCF1 or BAP1 (wild-type or F170I mutant) was confirmed by western blot analyses with anti-HA or anti-FLAG antibody. (b) Statistical analysis in triplicate, ubiquitination of HCF1. Statistical significance is indicated by the asterisk ($P < 0.05$, Student's *t*-test). (c) Deubiquitination of BAP1. Plasmids were transfected into HEK-293T cells. Cell extracts were immunoprecipitated with anti-BAP1 antibody, followed by western blot analysis with either anti-Myc or anti-BAP1. (d) Statistical analysis in triplicate, ubiquitination of BAP1. Statistical significance is indicated by the double asterisk ($P < 0.01$, Student's *t*-test).

BAP1 alterations on both alleles of this tumor, which accounts for the biallelic inactivation of *BAP1* gene. A faint peak observed in sequence data of this tumor likely represents contaminated residual non-cancerous DNA.

Twenty-seven ESCC cases were examined by MLPA analysis and the results indicated that *BAP1* locus was deleted as frequently as 52% (14 cases), as shown in Table 1.

Non-synonymous genetic alteration found in esophageal squamous cell carcinoma induces depleted deubiquitinase activity and cytosolic localization of BAP1. As this codon is located in the UCH domain, and phenylalanine at codon 170 is highly conserved across species (Fig. 1c,d), we evaluated its effect on the deubiquitinase activity of BAP1. We constructed FLAG-tagged wild-type BAP1 (FLAG-BAP1-Wt) and BAP1-F170I (FLAG-BAP1-F170I). Using an *in vivo* ubiquitination assay to measure the level of ubiquitinated host cell factor C1 (HCF1), quantified by densitometer as described above in independent triplicated experiments, we showed that deubiquitinase activity was

significantly depleted in the F170I mutant compared with wild-type BAP1 ($P < 0.05$). The expression level of FLAG-BAP1-F170I was confirmed to be similar to that of FLAG-BAP1-Wt (Fig. 2a,b).

The reduced deubiquitination of HCF1 suggested that auto-deubiquitinated BAP1 might be decreased. Then ubiquitinated BAP1 was also evaluated by anti-BAP1 IP followed by anti-Myc western analysis (Fig. 2c,d). Results obtained from triplicated experiments show that the level of ubiquitinated BAP1 significantly increased by F170I mutation ($P < 0.01$).

Auto-deubiquitinated BAP1 likely localizes within the nucleus because of the deubiquitinated nuclear localization signals within this protein.⁽⁵⁾ Hence, we investigated the subcellular localization of wild-type BAP1 and the F170I mutant. We transfected U2OS cells with FLAG-BAP1-Wt or FLAG-BAP1-F170I and stained them with anti-FLAG antibody. We showed that F170I mutant preferentially localized within the cyto-

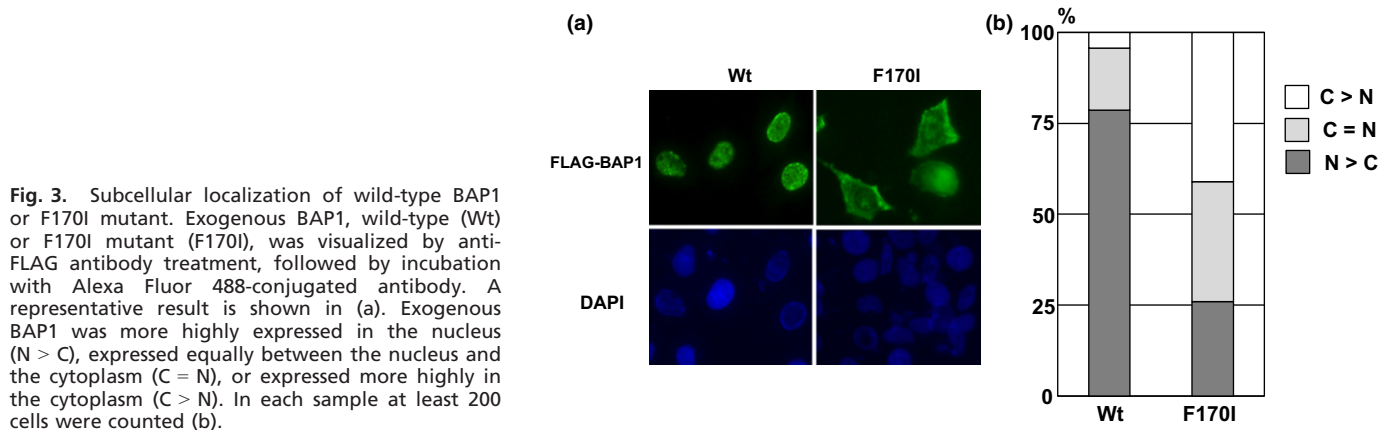


Fig. 3. Subcellular localization of wild-type BAP1 or F170I mutant. Exogenous BAP1, wild-type (Wt) or F170I mutant (F170I), was visualized by anti-FLAG antibody treatment, followed by incubation with Alexa Fluor 488-conjugated antibody. A representative result is shown in (a). Exogenous BAP1 was more highly expressed in the nucleus ($N > C$), expressed equally between the nucleus and the cytoplasm ($C = N$), or expressed more highly in the cytoplasm ($C > N$). In each sample at least 200 cells were counted (b).

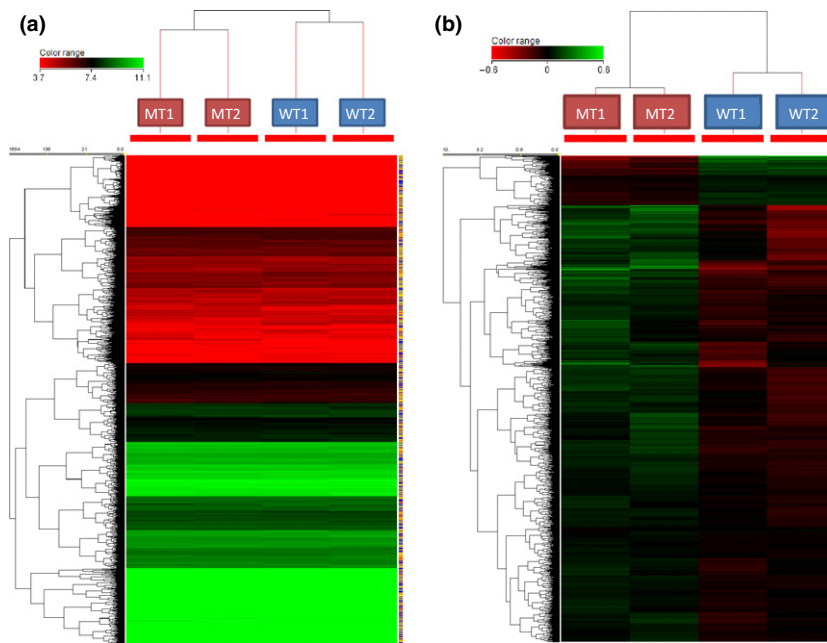


Fig. 4. Heat map analyses of gene expression profiles. MT and WT stand for F170I mutant and wild-type BAP1, respectively. Expression profiles were examined in two independent transfections, 1 or 2 (a). A total of 5840 genes, selected by principal component analysis from the values of the first component of the vector, excluding genes without genome annotation, were used for heat map analysis by adjusting the average expression level of each gene to 0 (b).

plasm, whereas wild-type BAP1 mostly localized within the nucleus (Fig. 3).

F170I mutant alters gene expression profiles relating to oncogenic pathways. HCF1 is a nuclear transcription coregulator that may be involved in cell cycle control through transcription regulation. Less deubiquitinated HCF1 might lead to drastic changes in terms of transcriptional regulation.⁽²⁾ Therefore, we examined gene expression profiles by microarray analysis. As shown in Figure 4(a), expression profiles were dramatically different between wild-type BAP1 and the F170I mutant; clustering analysis revealed that expression profiles could be classified into wild-type and the F170I mutant reproducibly in two independent transfections. This was confirmed by principal component analysis. Figure 4(b) shows the results of heat map analysis of 5840 genes that were identified by the first component of the vector in principal component analysis, by adjusting the averaged value of all probes to 0. Table 2 shows the results obtained for the 5840 genes selected above in gene-ontology analyses using four different programs. In general, this reproducibly contributed to the differentiation between wild-type BAP1 and the F170I mutant. Each result indicates that the expression of genes involved in oncogenic pathways was drastically altered by the expression of the F170I mutant compared with that of wild-type BAP1.

Nuclear BAP1 expression is lacking in 44% of esophageal squamous cell carcinoma. We found that nuclear BAP1 expression was absent in 23 out of 52 (44%) ESCCs examined by immunohistochemistry (Fig. 5a,b). Interestingly, 8 of these displayed strong cytosolic expression of BAP1 (Fig. 5c). The BAP1-nuclear negative tumors more likely lost the *BAP1* locus by CNV analysis than the BAP1-nuclear positive tumors; BAP1-nuclear negative tumors were found in 22% (2/9) of no-CNV tumors versus 67% (4/6) in *BAP1*-deleted tumors (Table 1).

A putative tumor suppressor, TCEAL7, is significantly induced by wild-type BAP1. Among multiple genes involved in oncogenic pathways, as shown in Table 2, we could confirm that the expression level of *TCEAL7* was significantly induced in wild-type BAP1-transfected HEK-293T cells as compared to F170I mutant transfected HEK-293T cells (Fig. 6).

Discussion

In the current study, we showed that *BAP1*, which is located on chromosome 3p21.3, was somatically altered in 1 tumor of 49 ESCCs examined, in which monoallelic deletion of *BAP1* gene was also detected by MLPA (Fig. 1). Furthermore, our results suggested that BAP1 might be functionally inactivated in 44% of ESCC by IHC analysis, because BAP1 has been reported to function within the nucleus and BAP1 was not expressed within the nucleus in 44% of ESCCs.^(3–5) Besides, the results of MLPA analysis showed that the monoallelic loss (LOH) of *BAP1* occurred as frequently as 52% in ESCC (Fig. 1b and Table 1). As MLPA was reported to be accurate compared to array CGH, fluorescence *in situ* hybridization, and gene copy number assay,⁽²⁶⁾ the results obtained in the current study suggested that the BAP1 gene and/or nearby genes are involved in the esophageal tumorigenesis. This view may be supported by our other results; these figures for BAP1-nuclear negative tumors and *BAP1* deletion are comparable and BAP1-nuclear negative tumors likely lost allele at *BAP1* locus more than BAP1-nuclear positive tumors.

As ESCC is one of the leading causes of cancer death worldwide, many genome analyses have been reported. Several genes that are mutated in ESCC have been described, including *TP53*, *CDKN2A*, *NOTCH1* and *NFE2L2*.^(27–30) The role of BAP1 in esophageal carcinogenesis remains unclear; *BAP1* mutation was not reported in 71 cases of ESCC examined by Song *et al.*,⁽³¹⁾ although two frameshift mutations in 113 cases were reported by Gao *et al.*⁽³²⁾ In the catalogue of genetic mutation in human cancer (the COSMIC database; <http://cancer.sanger.ac.uk/cancergenome/projects/cosmic/>), *BAP1* somatic mutation is reported in only one ESCC. Consistently, in the current study, we observed *BAP1* mutation in only 1 case of 49 examined. However, although it is rare, we believe that the somatic mutation of *BAP1* is a driver mutation of ESCC, at least in some cases, including the current one. This is because of our functional data that suggested the biallelic alteration of *BAP1* (Fig. 1a,b), the displayed less deubiquiti-

Table 2. Molecular pathways differentially induced by the F170I mutant

IPA canonical pathways			DAVID KEGG		DAVID Biocarts		DAVID Reactome	
Pathway	-log(P-value)	Pathway	P-value	Pathway	P-value	Pathway	P-value	
Molecular mechanisms of cancer	1.32E+01	Lysosome	1.70E-06	IL 6 signaling pathway	9.50E-03	Metabolism of proteins	3.00E-08	
Ephrin-B signaling	9.33E+00	Colorectal cancer	4.30E-04	Integrin signaling pathway	9.70E-03	Signalling by NGF	8.10E-07	
Ephrin receptor signaling	8.37E+00	Ribosome	4.40E-04	NFAT and hypertrophy of the heart (transcription in the broken heart)	1.10E-02	3' -UTR-mediated translational regulation	1.60E-05	
PI3K/AKT signaling	8.19E+00	Insulin signaling pathway	4.80E-04	Glycolysis pathway	2.00E-02	Diabetes pathways	1.60E-05	
Germ cell-sertoli cell junction signaling	7.92E+00	Adherens junction	1.50E-03	HIV-1 Nef	2.20E-02	Gene Expression	4.90E-05	
EIF2 signaling	7.66E+00	N-Glycan biosynthesis	1.70E-03	Links between Pyk2 and map kinases	2.30E-02	Influenza Infection	5.70E-05	
Pancreatic adenocarcinoma signaling	7.35E+00	Pathways in cancer	2.00E-03	Trefoil factors initiate mucosal healing	3.60E-02	HIV Infection	3.30E-04	
TGF-beta signaling	6.86E+00	Focal adhesion	4.00E-03	TGF beta signaling pathway	3.80E-02	Integration of energy metabolism	3.30E-04	
Axonal guidance signaling	6.37E+00	Chronic myeloid leukemia	4.10E-03	IL-2 receptor beta chain in T cell activation	3.90E-02	Signaling by TGF beta	1.30E-03	
Epithelial adherens junction signaling	6.33E+00	Wnt signaling pathway	5.20E-03	Regulation of transcriptional activity by PML	4.70E-02	Apoptosis	1.50E-03	
Sertoli cell-sertoli cell junction signaling	6.21E+00	p53 signaling pathway	6.60E-03	MAPKinase signaling pathway	4.90E-02	Signaling by Wnt	2.10E-03	
Wnt/beta-catenin signaling	6.13E+00	RNA polymerase	7.20E-03			Signaling by EGFR	2.20E-03	
Chronic myeloid leukemia signaling	6.04E+00	Small cell lung cancer	7.90E-03			Telomere Maintenance	1.30E-02	
Breast cancer regulation by stathmin 1	5.97E+00	Axon guidance	9.30E-03			Signaling by Insulin receptor	1.60E-02	
Cell cycle: G1/S checkpoint regulation	5.90E+00	Amino sugar and nucleotide sugar metabolism	1.30E-02			Transcription	1.80E-02	
Remodeling of epithelial adherens junctions	5.86E+00	TGF-beta signaling pathway	1.40E-02			Pausing and recovery of elongation	2.00E-02	
Cyclins and cell cycle regulation	5.84E+00	Pancreatic cancer	1.60E-02			Elongation arrest and recovery	2.00E-02	
14-3-3-mediated signaling	5.49E+00	MAPK signaling pathway	1.80E-02			HIV-1 elongation arrest and recovery	2.00E-02	
ERK/MAPK signaling	5.46E+00	Alzheimer's disease	1.80E-02			Pausing and recovery of HIV-1 elongation	2.00E-02	
Regulation of eIF4 and p70S6K signaling	5.36E+00	Neurotrophin signaling pathway	1.90E-02			Metabolism of carbohydrates	2.50E-02	
Androgen signaling	5.31E+00	Epithelial cell signaling in <i>Helicobacter pylori</i> infection	2.50E-02			Membrane Trafficking	2.70E-02	
ILK signaling	5.23E+00	RNA degradation	3.30E-02			Pausing and recovery of Tat-mediated HIV-1 elongation	3.50E-02	

Table 2 (continued)

IPA canonical pathways		DAVID KEGG		DAVID Biocarts		DAVID Reactome	
Pathway	-log(P-value)	Pathway	P-value	Pathway	P-value	Pathway	P-value
IGF-1 signaling	5.17E+00	Pathogenic Escherichia coli infection	3.30E-02			Tat-mediated HIV-1 elongation arrest and recovery	3.50E-02
PTEN signaling	5.10E+00	Non-small cell lung cancer	3.40E-02			Signaling by Notch	3.90E-02
CDK5 signaling	5.10E+00	Prostate cancer	3.50E-02			Signal attenuation	4.60E-02
Prostate cancer signaling	4.91E+00	Acute myeloid leukemia	4.10E-02				
mTOR signaling	4.88E+00	Endometrial cancer	4.30E-02				
Pyridoxal 5'-phosphate salvage pathway	4.84E+00	Glycosylphosphatidylinositol(GPI)-anchor biosynthesis	4.70E-02				
Integrin signaling	4.67E+00						
Protein ubiquitination pathway	4.65E+00						
Mouse embryonic stem cell pluripotency	4.59E+00						
Insulin receptor signaling	4.55E+00						
Mitochondrial dysfunction	4.43E+00						
Non-small cell lung cancer signaling	4.35E+00						
Cardiac hypertrophy signaling	4.26E+00						
Regulation of the epithelial-mesenchymal transition pathway	4.23E+00						
Amyloid processing	4.16E+00						
Acute myeloid leukemia signaling	4.00E+00						
Small cell lung cancer signaling	3.95E+00						
Colanic acid building blocks biosynthesis	3.94E+00						
Actin cytoskeleton signaling	3.93E+00						
Telomerase signaling	3.90E+00						
Salvage pathways of pyrimidine ribonucleotides	3.82E+00						
Phosphatidylglycerol biosynthesis II (non-plastidic)	3.71E+00						
IL-1 signaling	3.67E+00						
Myc mediated apoptosis signaling	3.55E+00						
Role of CHK proteins in cell cycle checkpoint control	3.53E+00						
Endometrial cancer signaling	3.51E+00						
CTLA4 signaling in cytotoxic T lymphocytes	3.48E+00						
Clathrin-mediated endocytosis signaling	3.38E+00						

Note: Pathways with $P < 0.05$ are listed except for the ingenuity pathways analysis (IPA) pathways, for which the top 50 pathways are listed.

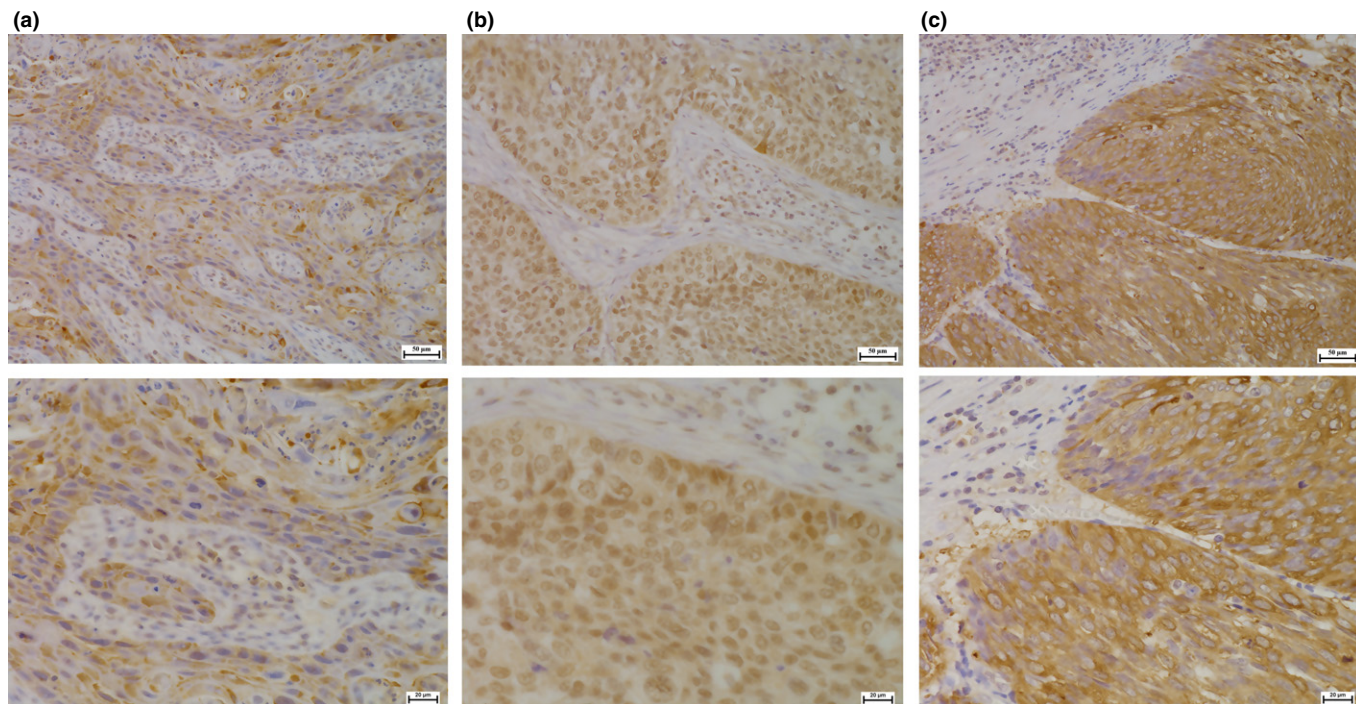


Fig. 5. Immunohistochemical staining of BAP1 in surgically resected esophageal cancer tissues. Representative features are shown, under low magnification (upper; bar 50 μm) and high magnification (lower; bar 20 μm). We classified (a) as BAP1 negative, (b) as BAP1-positive. In eight nuclear BAP1-negative cases, BAP1 was strongly expressed within the cytoplasm (c).

nase and auto-deubiquitinase activities (Fig. 2), a cytoplasmic localization (Fig. 3) and frequent nuclear BAP1-negative expressions in the esophageal cancers (Table 1). Besides, gene expression profiles in oncogenic pathways were markedly different between wild-type BAP1 and the F170I mutant (Fig. 4, Table 2). Furthermore, although F170I substitution has not been reported previously, F170V and F170L substitutions were

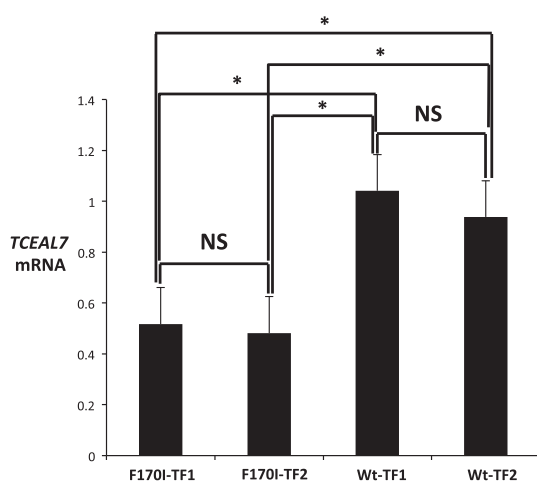


Fig. 6. Result of quantitative RT-PCR for *TCEAL7* expression in wild-type BAP1 or F170I mutant BAP1-transfected HEK-293T cells. RT-PCR was repeated in triplicate for duplicated transfections. Each asterisk indicates statistical significance ($P < 0.001$). TF1, TF2 and NS stand for transfection 1, transfection 2 and no statistical significance ($P = 1.0$ between TF1 and TF2 by F170I; $P = 0.43$ between TF1 and TF2 by Wt), respectively.

reported in renal cell carcinomas in the COSMIC database and by Pena-Llops *et al.*⁽⁹⁾ These results could support the view that amino acid substitution at codon 170 can be pathogenic. This is consistent with the fact that phenylalanine at codon 170 is highly conserved across species (Fig. 1d).

As described above, somatic mutation of the coding region of *BAP1* is rare in ESCC. However, our MLPA and IHC analyses revealed that the *BAP1* locus was deleted in ESCC as frequently as 52% and that nuclear expression of BAP1 was depleted in 44% of ESCC. Interestingly, 15 tumors out of 23 with depleted nuclear expression of BAP1 displayed no cytoplasmic expression (Table 1), consistent with previous IHC studies in melanoma,^(14,24) while the remaining 8 cases showed strong cytoplasmic expression of BAP1 instead (Fig. 5c). Recent IHC analysis showed that perinuclear localization of BAP1 is also observed in nuclear BAP1-negative sporadic epithelioid Spitz tumors; in that study, authors predicted that BAP1 in those tumors might result in the inability to be transported to the nucleus, trapped in the Golgi zone, which leads to an inability to perform its normal tumor suppressor function.⁽³³⁾

As previous studies suggest, BAP1 absent tumors, both in the nucleus and the cytoplasm, may harbor biallelic loss or somatic mutation with LOH of *BAP1*.^(24,34) However, the current study, we could not detect any somatic mutations in nuclear BAP1-negative ESCC in Table 1. This suggests that BAP1 may be inactivated mainly by pathways other than somatic mutation in nuclear BAP1-negative tumors. Gene deletion at large might explain these cases, as supported by the evidence in the current study (Table 1). Alternatively, UBE2O, which has been reported to suppress its function by recruiting BAP1 to the cytosol,⁽⁵⁾ is mutated in ESCC and in other esophageal carcinomas (see COSMIC data base).⁽³¹⁾ It is possible that altered UBE2O behaves as an oncoprotein like activated

EGFR or RAS family proteins. Therefore, BAP1 may be functionally inactivated in these cases with alterations of *UBE2O* or other genes involved in BAP1 ubiquitination, specifically in nuclear BAP1-negative but cytosolic positive tumors.

The detailed mechanism of carcinogenesis by BAP1-negative tumor has not been disclosed so far, but we could show one candidate in downstream of BAP1 by the current study: wild-type BAP1 significantly induces *TCEAL7* expression more than F170I mutant BAP1 (Fig. 6). *TCEAL7*, transcription elongation factor A-like 7, has been reported to induce apoptosis in ovarian cancer cells,⁽³⁵⁾ to negatively regulate Myc activity,^(26,36) to suppress nuclear factor (NF)- κ B binding to its target DNA sequences⁽³⁷⁾ and to induce p27 expression,⁽³⁸⁾ suggesting that *TCEAL7* behaves as a tumor suppressor.

Thus, BAP1 may play a key role in at least a part of esophageal carcinogenesis, not only by somatic mutation or gene deletion, but also by functional inactivation, such as by depleted deubiquitination or by cytoplasmic sequestration.

References

- Jensen DE, Proctor M, Marquis ST *et al.* BAP1: a novel ubiquitin hydrolase which binds to the BRCA1 RING finger and enhances BRCA1-mediated cell growth suppression. *Oncogene* 1998; **16**: 1097–112.
- Machida YJ, Machida Y, Vashisht AA, Wohlschlegel JA, Dutta A. The deubiquitinating enzyme BAP1 regulates cell growth via interaction with HCF-1. *J Biol Chem* 2009; **284**: 34179–88.
- Ventii KH, Devi NS, Friedrich KL *et al.* BRCA1-associated protein-1 is a tumor suppressor that requires deubiquitinating activity and nuclear localization. *Cancer Res* 2008; **68**: 6953–62.
- Misaghi S, Ottosen S, Izrael-Tomasevic A *et al.* Association of C-terminal ubiquitin hydrolase BRCA1-associated protein 1 with cell cycle regulator host cell factor 1. *Mol Cell Biol* 2009; **29**: 2181–92.
- Mashtalir N, Daou S, Barbour H *et al.* Autodeubiquitination protects the tumor suppressor BAP1 from cytoplasmic sequestration mediated by the atypical ubiquitin ligase UBE2O. *Mol Cell* 2014; **54**: 392–406.
- Harbour JW, Onken MD, Roberson ED *et al.* Frequent mutation of BAP1 in metastasizing uveal melanomas. *Science* 2010; **330**: 1410–3.
- Bott M, Brevet M, Taylor BS *et al.* The nuclear deubiquitinase BAP1 is commonly inactivated by somatic mutations and 3p21.1 losses in malignant pleural mesothelioma. *Nat Genet* 2011; **43**: 668–72.
- Yoshikawa Y, Sato A, Tsujimura T *et al.* Frequent inactivation of the BAP1 gene in epithelioid-type malignant mesothelioma. *Cancer Sci* 2012; **103**: 868–74.
- Pena-Llopis S, Vega-Rubin-de-Celis S, Liao A *et al.* BAP1 loss defines a new class of renal cell carcinoma. *Nat Genet* 2012; **44**: 751–9.
- Jia Y, Pawlik TM, Anders RA *et al.* Exome sequencing identifies frequent inactivating mutations in BAP1, ARID1A and PBRM1 in intrahepatic cholangiocarcinomas. *Nat Genet* 2013; **45**: 1470–3.
- Chan-On W, Nairismagi ML, Ong CK *et al.* Exome sequencing identifies distinct mutational patterns in liver fluke-related and non-infection-related bile duct cancers. *Nat Genet* 2013; **45**: 1474–8.
- Abdel-Rahman MH, Pilarski R, Cebulla CM *et al.* Germline BAP1 mutation predisposes to uveal melanoma, lung adenocarcinoma, meningioma, and other cancers. *J Med Genet* 2011; **48**: 856–9.
- Testa JR, Cheung M, Pei J *et al.* Germline BAP1 mutations predispose to malignant mesothelioma. *Nat Genet* 2011; **43**: 1022–5.
- Wiesner T, Obenaus AC, Murali R *et al.* Germline mutations in BAP1 predispose to melanocytic tumors. *Nat Genet* 2011; **43**: 1018–21.
- Carbone M, Ferris LK, Baumann F *et al.* BAP1 cancer syndrome: malignant mesothelioma, uveal and cutaneous melanoma, and MIBAITs. *J Transl Med* 2012; **10**: 179.
- Carbone M, Yang H, Pass HI, Krausz T, Testa JR, Gaudino G. BAP1 and cancer. *Nat Rev Cancer* 2013; **13**: 153–9.
- Pilarski R, Cebulla CM, Massengill JB *et al.* Expanding the clinical phenotype of hereditary BAP1 cancer predisposition syndrome, reporting three new cases. *Genes Chromosom Cancer* 2013; **53**: 177–82.
- de la Fouchardiere A, Cabaret O, Savin L *et al.* Germline BAP1 mutations predispose also to multiple basal cell carcinomas. *Clin Genet* 2014; doi: 10.1111/cge.12472.

Although further analysis is needed, BAP1 may be a useful therapeutic target in ESCC.

Acknowledgments

The authors are grateful to Professor Yataro Daigo (Shiga University of Medical Science) for his careful reading of this manuscript and advice, and to Dr Yuki Yoshino (Tohoku University) and Hidenori Sato (Yamagata University) for their technical contributions on molecular biological experiments. This work was supported by a grant-in-aid for scientific research C, #25462010, from the Ministry of Education, Culture, Sports, Science and Technology, Japan, and the Program for interdisciplinary research in Frontier Research Institute for Interdisciplinary Sciences (FRIS), Tohoku University.

Disclosure Statement

The authors have no conflict of interest to declare.

- Aoki T, Mori T, Du X, Nishihira T, Matsubara T, Nakamura Y. Allelotyping study of esophageal carcinoma. *Genes Chromosom Cancer* 1994; **10**: 177–82.
- Mori T, Yanagisawa A, Kato Y *et al.* Accumulation of genetic alterations during esophageal carcinogenesis. *Hum Mol Genet* 1994a; **3**: 1969–71.
- Okano S, Kanno S, Nakajima S, Yasui A. Cellular responses and repair of single-strand breaks introduced by UV damage endonuclease in mammalian cells. *J Biol Chem* 2000; **275**: 32635–41.
- Starita LM, Horwitz AA, Keogh MC, Ishioka C, Parvin JD, Chiba N. BRCA1/BARD1 ubiquitinate phosphorylated RNA polymerase II. *J Biol Chem* 2005; **280**: 24498–505.
- Govers R, van Kerkhof P, Schwartz AL, Strous GJ. Linkage of the ubiquitin-conjugating system and the endocytic pathway in ligand-induced internalization of the growth hormone receptor. *EMBO J* 1997; **16**: 4851–8.
- Wiesner T, Murali R, Fried I *et al.* A distinct subset of atypical Spitz tumors is characterized by BRAF mutation and loss of BAP1 expression. *Am J Surg Pathol* 2012; **36**: 818–30.
- Chien J, Narita K, Rattan R *et al.* A role for candidate tumor-suppressor gene *TCEAL7* in the regulation of c-Myc activity, cyclin D1 levels and cellular transformation. *Oncogene* 2008; **27**: 7223–34.
- Homig-Holzel C, Savola S. Multiplex ligation-dependent probe amplification (MLPA) in tumor diagnostics and prognostics. *Diagn Mol Pathol* 2012; **21**: 189–206.
- Hollstein MC, Metcalf RA, Welsh JA, Montesano R, Harris CC. Frequent mutation of the p53 gene in human esophageal cancer. *Proc Natl Acad Sci USA* 1990; **87**: 9958–61.
- Mori T, Miura K, Aoki T, Nishihira T, Mori S, Nakamura Y. Frequent somatic mutation of the MTS1/CDK4I (multiple tumor suppressor/cyclin-dependent kinase 4 inhibitor) gene in esophageal squamous cell carcinoma. *Cancer Res* 1994b; **54**: 3396–7.
- Agrawal N, Jiao Y, Bettgowda C *et al.* Comparative genomic analysis of esophageal adenocarcinoma and squamous cell carcinoma. *Cancer Discov* 2012; **2**: 899–905.
- Abedi-Ardekani B, Hainaut P. Cancers of the upper gastro-intestinal tract: a review of somatic mutation distributions. *Arch Iran Med* 2014; **17**: 286–92.
- Song Y, Li L, Ou Y *et al.* Identification of genomic alterations in oesophageal squamous cell cancer. *Nature* 2014; **509**: 91–5.
- Gao YB, Chen ZL, Li JG *et al.* Genetic landscape of esophageal squamous cell carcinoma. *Nat Genet* 2014; **46**: 1097–102.
- Gammon B, Traczyk TN, Gerami P. Clumped perinuclear BAP1 expression is a frequent finding in sporadic epithelioid Spitz tumors. *J Cutan Pathol* 2013; **40**: 538–42.
- Koopmans AE, Verdijk RM, Brouwer RW *et al.* Clinical significance of immunohistochemistry for detection of BAP1 mutations in uveal melanoma. *Mod Pathol* 2014; **27**: 1321–30.
- Chien J, Staub J, Avula R *et al.* Epigenetic silencing of *TCEAL7* (*Bex4*) in ovarian cancer. *Oncogene* 2005; **24**: 5089–100.
- Lafferty-whyte K, Bilstand A, Hoare SF *et al.* *TCEAL7* inhibition of c-Myc activity in alternative lengthening of telomeres regulates hTERT expression. *Neoplasia* 2010; **12**: 405–14.

- 37 Rattan R, Narita K, Chien J *et al.* TCEAL7, a putative tumor suppressor gene, negatively regulates NF- κ B pathway. *Oncogene* 2010; **29**: 1362–73.
- 38 Shi X, Garry DJ. Myogenic regulatory factors transactivate the *Tceal7* gene and modulate muscle differentiation. *Biochem J* 2010; **428**: 213–21.

Supporting Information

Additional supporting information may be found in the online version of this article:

Table S1. BAP1-primers: Sequences of the primers used to amplify and to sequence each exon.